Biophysical Chemistry 163–164 (2012) 44–55

Contents lists available at SciVerse ScienceDirect

Biophysical Chemistry

journal homepage: http://www.elsevier.com/locate/biophyschem

On the temperature stability of extracellular hemoglobin of *Glossoscolex paulistus*, at different oxidation states: SAXS and DLS studies

José Wilson P. Carvalho [a], Patrícia S. Santiago [a,b], Tatiana Batista [a], Carlos Ernesto Garrido Salmon [c], Leandro R.S. Barbosa [d], Rosangela Itri [d], Marcel Tabak [a,*]

[a] *Instituto de Química de São Carlos, Universidade de São Paulo/São Carlos, SP, Brazil*
[b] *Campus experimental de Registro, Universidade Estadual Paulista "Júlio de Mesquita Filho"/Registro/SP, Brazil*
[c] *Departamento de Física, Faculdade de Filosofia Ciências e Letras de Ribeirão Preto, Universidade de São Paulo, Ribeirão Preto, SP, Brazil*
[d] *Instituto de Física, Universidade de São Paulo-São Paulo, SP, Brazil*

HIGHLIGHTS

- ► *Glossoscolex paulistus* hemoglobin (HbGp) was studied by DLS and SAXS.
- ► The thermal stability order is cyanomet->, oxy->, met-HbGp, at several pH values.
- ► Analyses of SAXS experimental curves were performed by GNOM and OLIGOMER.
- ► Experimental p(r) curves were anayzed by a linear combination of HbLt fragments.
- ► Contributions from smaller fragments were observed at higher pH and temperature.

GRAPHICAL ABSTRACT

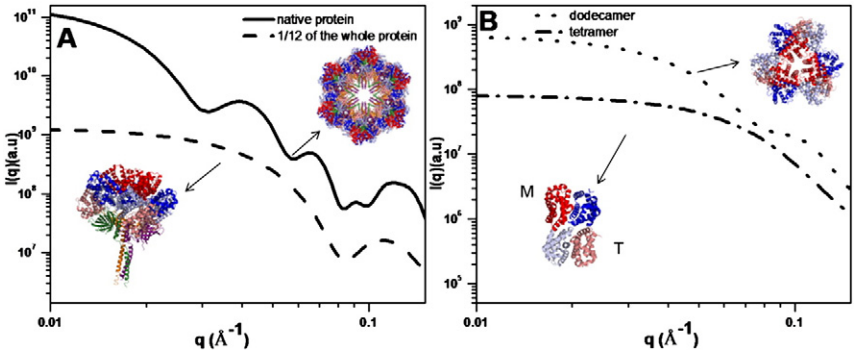

ARTICLE INFO

Article history:
Received 9 December 2011
Received in revised form 4 February 2012
Accepted 6 February 2012
Available online 16 February 2012

Keywords:
Extracellular hemoglobin
Glossoscolex paulistus
Oligomeric dissociation
Thermal stability
DLS
SAXS

ABSTRACT

Glossoscolex paulistus hemoglobin (HbGp) was studied by dynamic light scattering (DLS) and small angle X-ray scattering (SAXS). DLS melting curves were measured for met-HbGp at different concentrations. SAXS temperature studies were performed for oxy-, cyanomet- and met-HbGp forms, at several pH values. At pH 5.0 and 6.0, the scattering curves are identical from 20 to 60 °C, and R_g is 108 Å, independent of the oxidation form. At pH 7.0, protein denaturation and aggregation occurs above 55 °C and 60 °C, for oxy and met-HbGp, respectively. Cyanomet-HbGp, at pH 7.0, is stable up to 60 °C. At alkaline pH (8.0–9.0) and higher temperature, an irreversible dissociation process is observed, with a decrease of R_g, D_{max} and I(0). Analysis by p(r), obtained from GNOM, and OLIGOMER, was used to fit the SAXS experimental scattering curves by a combination of theoretical curves obtained for HbLt fragments from the crystal structure. Our results show clearly the increasing contribution of smaller molecular weight fragments, as a function of increasing pH and temperature, as well as, the order of thermal stabilities: cyanomet- > oxy- > met-HbGp.

1. Introduction

Extracellular annelid hemoglobins are giant molecules that have a characteristic two-disk hexagonal bilayer (HBL) as shown by electron micrographs [1]; they exhibit high cooperativity of oxygen binding and heme contents [2–4]. Due to their extracellular nature, large size and resistance to oxidation, erythrocruorins have been proposed as useful model systems for developing therapeutic blood substitutes and preliminary animal experiments have been encouraging [5].

The extracellular hemoglobin of *Glossoscolex paulistus* (HbGp) is an oligomeric protein constituted by subunits containing heme

* Corresponding author. Fax: +55 16 3373 9982.
E-mail address: marcel@sc.usp.br (M. Tabak).

0301-4622/$ – see front matter © 2012 Elsevier B.V. All rights reserved.
doi:10.1016/j.bpc.2012.02.004

groups, monomers and trimers, and non-heme structures, named linkers. The whole protein has a molecular mass of 3.6×10^6 Da [6], being homologous to *Lumbricus terrestris* hemoglobin (HbLt) [7] that is the most extensively studied annelid hemoglobin.

In recent years, some papers have described the dissociation mechanisms of this class of proteins. Analysis by analytical ultracentrifugation (AUC) of HbGp solution in the oxy- and cyanomet-forms, at pH 10.0, has shown the existence of several species in equilibrium [8]. For oxy-HbGp four species were observed, which were assigned to the following subunits: subunit *d*, dimers of subunit *d*, d_2, trimers *abc* and a fourth species associated, probably, to the tetramer *abcd*. No contribution from undissociated integral protein was observed, suggesting that, at pH 10.0, the reduced form of the hemoglobin is completely dissociated. However, for cyanomet-HbGp, 17% of the protein remains in the native undissociated form, suggesting a higher oligomeric stability of the oxidized cyanomet form in alkaline medium.

In a previous work, we made use of small angle X-ray scattering (SAXS) experiments [9] and investigated the structural conformation of the HbGp in the oxy- and met-forms in the absence and presence of anionic surfactant SDS, at pH 7.0 and 9.0. At pH 7.0 and 25 °C, the SAXS curves were consistent with HBL structure, resulting in R_g and D_{max} values of 110 Å and 300 Å, respectively. In the presence of 20 mM of SDS and/or at alkaline pH of 9.0 R_g and D_{max} decreased, suggesting oligomeric dissociation. However, this previous work did not include the temperature effect on the denaturation and dissociation of HbGp in the different iron oxidation forms (oxy, met and cyanomet), and the effect of pH in the acidic range, where according to recent dynamic light scattering (DLS) data the oligomeric stability is very high [10,11].

The thermal stability of HbGp was addressed in our recent work, and DLS experiments have shown that oxy-HbGp is very stable up to 52 °C, at pH 7.0, presenting a hydrodynamic diameter of 27–28 nm [11]. Above 52–54 °C, oxy-HbGp denatured with formation of large size aggregates with D_h of 300 nm. In acid solution, in the pH range from 5.0 to 7.0, the protein is also very stable and upon denaturation, at somewhat higher temperatures (around 56 °C) as compared to pH 7.0, a stronger aggregation is observed, forming large aggregates with hydrodynamic radius of 3000 nm (at pH 6.1). On the other hand, at alkaline pH, the oxy-HbGp undergoes oligomeric dissociation upon temperature increase. The critical dissociation temperature changes from 44 to 32 °C upon increasing the pH from 7.5 to 8.3; further increase in temperature leads to denaturation and moderate aggregation [11]. More recently, studies on the thermal denaturation of oxy- and cyanomet-HbGp monitored by differential scanning calorimetry (DSC) and DLS were reported, where for the first time some thermodynamic parameters were obtained for HbGp at pH 7.0 and 8.0 [10]. These studies also show that cyanomet-HbGp is more stable than the oxy-form, and both HbGp oxidation forms have high activation energies for denaturation, at pH 7.0 and 8.0. These DSC studies also indicate that oxy-HbGp, at alkaline pH, undergoes oligomeric dissociation before denaturation. Besides, the HbGp thermal denaturation process is dependent on the protein concentration, and the denaturation temperature shifts to a higher value upon increase of protein concentration [10].

In the current work, we extend our previous investigation and study the thermal stability of HbGp in different oxidation states and in the range of pH acid, neutral and alkaline, by SAXS and dynamic light scattering.

2. Materials and methods

2.1. Purification and preparation of HbGp

The hemoglobin of *G. paulistus* was prepared using freshly drawn blood from worms as described earlier [11–14]. The blood sample was centrifuged at 4 °C ($2300\times g$ for 15 min) to eliminate cell debris. An ultra-filtration (molecular mass cut-off 30 kDa) in 0.1 M Tris–HCl buffer pH 7.0, at 4 °C, was performed in order to eliminate low M_w components. After the ultracentrifugation at $250{,}000\times g$, at 4 °C, during 3 h, HbGp is obtained as a pellet and then resuspended in a minimum amount of 0.1 M Tris–HCl buffer pH 7.0 and stored in the oxy-form at 4 °C. Chromatography at pH 7.0 in a Sephadex G-200 column furnished the samples used in our experiments. All concentrations were determined spectrophotometrically in a Shimadzu 1601PC spectrophotometer, using the molar extinction coefficients $\varepsilon_{415nm}=5.5\pm0.8\,(mg/ml)^{-1}\,cm^{-1}$ for oxy-HbGp, $\varepsilon_{402nm}=4.1\pm0.5\,(mg/ml)^{-1}\,cm^{-1}$ for met-HbGp and $\varepsilon_{420nm}=4.8\pm0.5\,(mg/ml)^{-1}\,cm^{-1}$ for cyanomet-HbGp [11,14]. The samples used for SAXS experiments were prepared, in general, 24–48 h prior to the measurements.

2.2. DLS measurements

The commercial instrument Zetasizer Nano ZS (Malvern, UK) was used on the light scattering measurements for particle size determination. This instrument allows dynamic light scattering measurements incorporating noninvasive backscattering (NIBS) optics. A He–Ne laser has been used as a light source with wavelength $\lambda=633$ nm. The intensity of light scattered at an angle of 173° is measured by an avalanche photodiode. The solutions were placed in the thermostated sample chamber that is temperature regulated for measurements over an interval from 25 to 70 °C, controlled with an accuracy of 0.1 °C. At each temperature seven measurements are performed and for each one a number of measurements are taken (normally around ten) to obtain an adequate statistics. The instrument measures the time dependent intensity fluctuation of light scattered from the particles in solution. Malvern's DTS software analyzes the acquired correlogram (correlation function vs. time plot) for the calculation of the hydrodynamic diameter, D_h. Hydrodynamic diameters of the particles were estimated from the autocorrelation function, using the Cumulant's method based on a single exponential fit of the correlation function to obtain the mean size (Z-average diameter) and an estimate of the width of the distribution (polydispersity index — PDI). These experiments were performed using met- and cyanomet-HbGp concentrations in the range from 0.5 to 3 mg/ml at pH 7.0 to 8.0. Additional melting experiments for met-HbGp, at pH 5.0, were performed at several protein concentrations, in the range from 0.5 to 3.0 mg/ml.

2.3. Optical absorption measurements

Samples of met-HbGp 3.0 mg/ml were subjected to heating, maintaining them at 50, 60 and 70 °C, for 1 h, with subsequent cooling down to room temperature (25 °C). After this heating cycle, all samples were centrifuged at 5000 rpm, collecting the supernatant for spectral analysis, in the range between 250 and 700 nm. The amount of protein remaining in solution was estimated based on the absorbance values at 403 nm, as compared to the sample maintained at 25 °C.

2.4. SAXS measurements

Solutions with protein concentrations at 3.0 mg/ml were measured as a function of temperature and pH values for different protein oxidation forms (oxy-, cyanomet- and met-HbGp) for 5 min exposure time and recorded in a 2-dimensional position sensitive detector MARCCD. SAXS experiments were performed at the National Synchrotron Light Laboratory, Campinas, Brazil, using a detector–sample distance of 1500 mm. The scattering vector amplitude q is defined as $q=4\pi\sin\theta/\lambda$, 2θ being the scattering angle and λ the X-ray wavelength of 1.608 Å [15]. Scattering curves were recorded within the q range from 0.01 to 0.25 $Å^{-1}$. According to the sampling theorem [15], the maximum dimension of scattering particle that could be

achieved was circa 628 Å ($D_{max} = 2\pi/q_{min}$). The experimental intensities were corrected for sample's attenuation, detector homogeneity, and buffer scattering.

2.5. SAXS data analyses

In the absence of interference effects, a Fourier transform connects the scattering intensity I(q) to the pair distance distribution function, p(r), which is related to the probability of finding a pair of small elements at a distance r within the entire volume of the scattering particle [15,16]. This is a model-independent function that provides information about the scattering particle maximum dimension, D_{max}, its radius of gyration, R_g, and its shape.

In this work, we made use of the GNOM program [17] to calculate p(r) functions from the theoretical and experimental scattering curves and the respective R_g values (see Tables 2–4). Considering that SAXS measurements are made in a limited q range, between q_{min} and q_{max}, and assuming the validity of the Guinier approximation, the intensity I(q) below q_{min} was extrapolated to I(0) [18,19]. It is important to mention that at $q_{max} = 0.25$ Å^{-1} HbGp scattering intensity is very similar to the scattering of the buffer.

Furthermore, we also performed a non-linear fitting (*Origin* 8.0 software) between the obtained p(r) functions at a given temperature and pH conditions, and a linear combination of the p(r) functions correspondent to the scattering of the fragments (subunits) of the protein. The scattering curves for the fragments were obtained from HbLt crystal structure (PDB under ID code 2GTL [7]) by using the CRYSOL software [18]. The use of HbLt structure as a model for HbGp, both in the native form and in the smaller fragments, seems reasonable due to the fact that both proteins present a similar molecular mass (3.6 MDa), as well as an oligomeric dissociation equilibrium, involving the co-existence of multiple species, and also the similarity in structure [6,7,9,20]. Moreover, the monomeric HbGp globin chain (d) has been fully sequenced [21] and presents 57% amino acid sequence identity with its homologue HbLt, indicating a common evolutionary origin [21]. Since the complete sequence is only known for the HbGp monomeric chain (d), at the present time it is yet not possible to obtain the complete resolution of HbGp structure. We consider that this fit in the r-space is more intuitive to monitor the size changes.

2.6. Molecular weight determination

From I(0) values, we evaluated the molecular weight, M, of the scattering particles by means of SAXSMoW software [19], which allowed us to determine *M* from SAXS data measured on a relative scale [19].

The *M* value obtained for the native protein is very close to the literature [6]. However, the values obtained for the dissociated systems are only a crude approximation, since this program was applied under the assumption of monodisperse systems, which is certainly not true.

2.7. Multimeric state analysis

In this work, we made use of the OLIGOMER package [18] to evaluate the percentage of dissociated and aggregated species in equilibrium in solution, depending on pH and temperature. The scattering data is considered as a linear combination of the species (components) present in solution according to the equation:

$$I(q) = \sum_{k=1}^{k} v_k I_k(q) \quad (1)$$

where v_k and $I_k(q)$ are the volume fraction and the scattering intensity from the *k*-th component, respectively, and the sum is over all components in the solution [18].

As the initial set of species, we used the results obtained from the analysis of the p(r) function. This will be better explained in Section 3.4.

3. Results and discussion

3.1. Thermal stability of HbGp, as a function of pH and iron oxidation state, monitored by DLS

3.1.1. Met-HbGp

The hydrodynamic diameter of the met-HbGp, estimated from DLS data, is shown in Fig. 1, for different pH values and protein concentrations. For met-HbGp, at 25 °C, at pH 7.0 (Fig. 1A) and 7.5 (Fig. 1B), the protein is in its native oligomeric form, showing a significant stability upon heating. The Z-average diameter of the met-HbGp 0.5 mg/ml, followed during 24 h, at 25 °C and pH 7.0, was 27 ± 1 nm. At pH 7.5, a slight reduction of diameter is observed at 24 ± 1 nm after 24 h. However, at pH 8.0 and 25 °C, an initial protein dissociation is observed. The average polydispersity indexes observed for met-HbGp, at pH values 7.0, 7.5 and 8.0 are, respectively, 0.01, 0.11 and 0.19. In a previous work we associated the increase of polydispersion indexes with the phenomenon of oxy-HbGp oligomeric dissociation [11].

At pH 7.0, where HbGp is very stable in all three oxidation forms (oxy, met and cyanomet), the increase in the temperature does not induce the dissociation of the protein (see inset in Fig. 1A, [11]). However, when a high temperature is reached (48 °C, Fig. 1A, Table 1) protein denaturation occurs, followed by some protein aggregation, as judged by the formation of a complex with a Z-average, $\langle D_h \rangle$, of 194 nm for 0.5 mg/ml at the highest temperature (Table 1). As mentioned above, a critical denaturation temperature (T_{den}) for

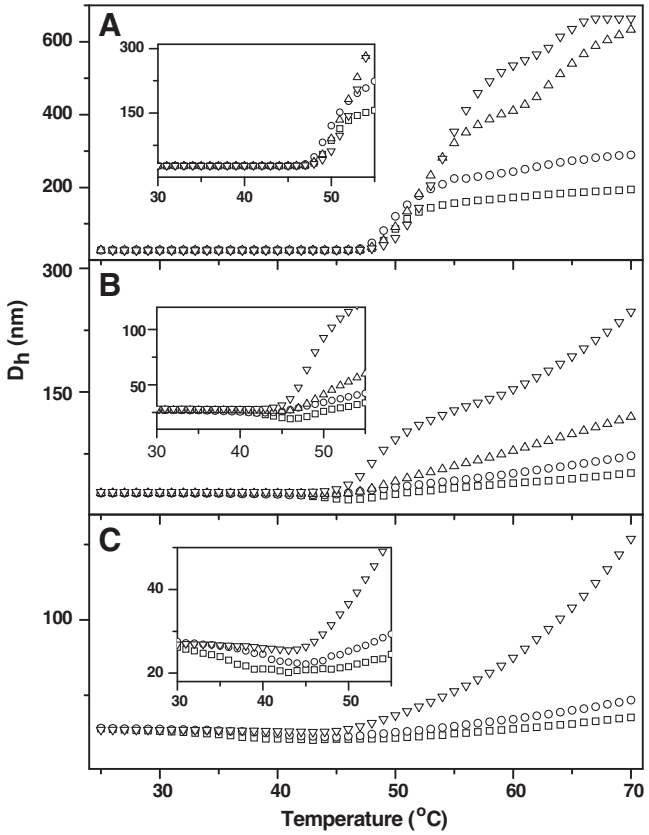

Fig. 1. Effect of temperature on the met-HbGp hydrodynamic radius at different protein concentrations and pH values. The buffers used were acetate–phosphate–borate 30 mM, at pH 7.0 (A), 7.5 (B) and 8.0 (C). The insets highlight the plots, between 30 and 55 °C, to show the partial oligomeric dissociation, at pH 7.5 and 8.0, and the high stability at pH 7.0. Protein concentrations are 0.5 (squares), 1.0 (circles), 2.0 (triangles) and 3.0 (inverted triangles) mg/ml, respectively.

met-HbGp was defined at 48 °C and pH 7.0, where the scattering particle dimension changed drastically, suggesting the appearance of aggregates in solution as a result of the denaturation process. The increase of protein concentration did not alter the T_{den} value for met-HbGp, at pH 7.0 (inset in Fig. 1A, Table 1). Nevertheless, an increase in the $<D_h>$ for the aggregates is observed as the protein concentration increases, which is a common phenomenon for all pH values in the range 7.0–8.0. So, higher protein concentrations induced the formation of larger aggregates (Fig. 1), independent of pH. Note, however, that the mechanisms of protein dissociation and aggregation have different pathways depending on pH value [10,11,14]. First of all, in going to acidic pH range, closer to the protein pI, which is 5.5 [14], the protein becomes more prone to aggregate. In this way, upon going to lower pH values the aggregation/precipitation becomes more prominent. This is clearly seen in the melting curves for met-HbGp, at pH 5.0, shown in Fig. S1 of the Supplementary data. Besides, in going to the opposite direction, alkaline pH, the protein undergoes oligomeric dissociation, which in turn affects the aggregation process and reduces the precipitation phenomenon and limits the sizes of the aggregates. It is worthy of notice, that the higher the pH value the lower the size of the aggregates attained at the highest temperatures (Table 1, Fig. 1).

At pH 7.5 and 0.5 and 1.0 mg/ml of protein, a slight decrease of $<D_h>$ is associated to the temperature induced protein oligomeric dissociation, followed by an increase of $<D_h>$, which is gradual and starts at a higher temperature, as compared to the temperature for protein dissociation (see inset in Fig. 1B). The temperatures at the beginning of the dissociation and denaturation processes (T_{diss} and T_{den}, respectively) are included in Table 1. It is clear that the dissociation is not complete since $<D_h>$ values are higher than that expected for oligomeric dissociation (around 10 nm, [10,11]), and that the beginning of the denaturation overlaps with the dissociation process. Table 1 also includes the minimal $<D_h>$ values observed in the melting curves (inset in Fig. 1B). At higher protein concentrations, 2.0 and 3.0 mg/ml, the dissociation phenomenon is not observed. It is interesting to notice that, in going from pH 7.0 to pH 7.5, T_{den}, for met-HbGp, reduces from 48 °C to 44 °C (Table 1).

At pH 8.0, for met-HbGp, the thermal stability is reduced as compared to pH 7.0. In the protein concentration range from 0.5 to 3.0 mg/ml, a slight decrease of $<D_h>$ is also observed (inset in Fig. 1C). The oligomeric dissociation is also not complete ($<D_h>$ values are higher than 10 nm) and the beginning of the denaturation overlaps again with the dissociation process. The lowest value of $<D_h>$ at pH 8.0 (25 nm) is also higher than that observed for oxy-HbGp, which is around 12 nm corresponding to a more extensive oligomeric dissociation [10,11].

Complimentary experiments were also performed for met-HbGp, at pH 5.0 and 7.0, to investigate the influence of the protein concentration on its thermal denaturation. Firstly, a DLS study was made, changing the protein concentration in the range from 0.5 to 2.0 mg/ml, at pH 5.0 (Fig. S1, Table S1), to compare with the results shown in Fig. 1 (for pH 7.0). The melting curves (Fig. S1) present a change of D_h from the very beginning of the heating cycle, suggesting that some slight protein aggregation takes place upon heating met-HbGp, at pH 5.0. After the completion of the melting experiment a very significant amount of precipitated protein is observed in the sample cuvette. Besides, as can be noticed in Fig. S1 and Table S1, the $<D_h>$ values increase significantly, at the highest temperatures, in the heating cycle. This makes it quite difficult to make some reliable assessment of aggregate size during this experiment. The critical denaturation temperatures are also higher at pH 5.0 (Table S1) as compared to pH 7.0 (Table 1), being around 60 °C, consistent with previous findings for oxy- [11] and cyanomet-HbGp [10].

Using optical absorption spectroscopy, another experiment was performed with met-HbGp, aiming to estimate the amount of aggregate/precipitate, at pH 5.0 and 7.0, produced upon heating the protein, at 50, 60 and 70 °C (Fig. S2). The results show that, at pH 5.0 (Fig. S2A) a significant amount of hemichrome is formed at 25 °C. After heating to 50 or 60 °C, around 9% of protein precipitation is observed, while, at 70 °C, a higher aggregation/precipitation of around 40% of protein takes place (Fig. S2A, Table S2). This observation is consistent with previous studies [10,11,14]. Moreover, at pH 7.0, it is clear that met-HbGp undergoes a change into hemichrome upon heating above 25 °C (Fig. S2B). The amount of protein remaining in solution after the heating cycle is quite similar to that observed at pH 5.0, even though the final aggregate size at the acidic pH seems to be much higher as compared to the neutral pH. These findings illustrate the fact that differences are found for the dissociation/aggregation phenomena at acidic and neutral pH. Since the protein aggregation is not the focus of the present work it will be a very interesting matter for future research.

Table 1
Values of the sizes and critical temperatures associated to the effects of pH, temperature and protein concentration on met- and cyanomet-HbGp. Z-average hydrodynamic diameter ($<D_h>$) at different pH values. The melting points were obtained from the data in Fig. 1.

[HbGp] mg/ml	T_{diss} (°C)	$<D_h>_{diss}$ (nm)	$<D_h>_{min}$ (nm)	T_{den}(°C)	$<D_h>_{den}$(nm)
			Met-HbGp		
			pH 7.0		
0.5	–	–	–	48 ± 1	194 ± 7
1.0	–	–	–	47 ± 1	288 ± 10
2.0	–	–	–	48 ± 1	632 ± 15
3.0	–	–	–	48 ± 1	664 ± 20
			pH 7.5		
0.5	40 ± 1	27 ± 1	19 ± 1	45 ± 1	52 ± 2
1.0	38 ± 1	27 ± 1	24 ± 1	44 ± 1	73 ± 3
2.0	–	–	–	44 ± 1	119 ± 5
3.0	–	–	–	44 ± 1	248 ± 8
			pH 8.0		
0.5	25 ± 1	26 ± 1	20 ± 1	44 ± 1	35 ± 1
1.0	25 ± 1	27 ± 1	22 ± 1	45 ± 1	47 ± 2
3.0	34 ± 1	27 ± 1	25 ± 1	43 ± 1	153 ± 5
			Cyanomet-HbGp		
			pH 7.0		
0.50	–	–	–	56 ± 1	100 ± 5
1.0	–	–	–	56 ± 1	123 ± 4
2.0	–	–	–	56 ± 1	138 ± 7
3.0	–	–	–	56 ± 1	690 ± 12
			pH 8.0		
0.50	42 ± 1	27 ± 1	16 ± 1	51 ± 1	29 ± 2
1.0	43 ± 1	27 ± 1	17 ± 1	52 ± 1	36 ± 3
2.0	45 ± 1	27 ± 1	19 ± 1	52 ± 1	53 ± 4
3.0	49 ± 1	27 ± 1	23 ± 1	56 ± 1	70 ± 5

T_{diss} critical dissociation temperature (beginning of the dissociation process); T_{den} critical denaturation temperature (beginning of the denaturation process); $<D_h>_{diss}$ Z-average hydrodynamic diameter at the beginning of the dissociation; $<D_h>_{den}$ Z-average hydrodynamic diameter at the highest temperature (70 °C), $<D_h>_{min}$ Z-average hydrodynamic diameter at the minimum of the melting curves.

3.1.2. Cyanomet-HbGp

Similar DLS melting experiments were performed for cyanomet-HbGp, at pH 7.0 and 8.0. In Table 1 the corresponding results are also included. The melting curves for both oxidized forms of HbGp, met and cyanomet, are very similar, showing the same protein concentration trends.

Cyanomet-HbGp at pH 7.0 is very stable, and increase in the temperature does not induce protein dissociation. However, when a high temperature is reached (56 °C) protein denaturation occurs, followed by some protein aggregation. At pH 8.0, the protein becomes more stable at higher concentrations, as monitored by the increase in T_{diss} with the increase in protein concentration (Table 1). Regarding protein aggregation beyond the denaturation, the trend at pH 8.0 is similar to that at pH 7.0: the higher the protein concentration the higher the size of the aggregates. The corresponding values of critical parameters are also shown in Table 1. At pH 7.0, and differently from

oxy-HbGp [10], for the cyanomet-form the increase in protein concentration is not accompanied by any change in the value of T_{den}.

It is important, that lowering the temperature back to 25 °C, after heating to 70 °C, does not lead to a change in the final value of $<D_h>$ indicating that the temperature induced protein dissociation is an irreversible process for all HbGp forms studied in this work.

The higher critical denaturation and dissociation temperatures indicate that cyanomet-HbGp is more stable than both the oxy- [10,11] and the met-HbGp. At pH 7.0, the denaturation temperature for cyanomet-HbGp (Table 1) is also higher as compared to oxy-HbGp [10,11] and met-HbGp. This observation is in agreement with previous work on oxidized HbGp [12–14].

Our present results based on DLS for melting of HbGp at different pH values and protein concentrations, for different protein oxidation forms (met-, and cyanomet-HbGp), suggest that the effects of protein concentration on the thermostability are similar to those reported previously for oxy-HbGp [11], but not identical. Met-HbGp, for instance, seems to have a higher tendency to aggregate at pH 7.0 as compared to oxy- [11] and cyanomet-HbGp, as judged by the larger sizes of the aggregates and relatively small dependence of denaturation temperatures on the protein concentration (Table 1).

We now focus our attention on SAXS measurements performed on 3.0 mg/ml HbGp at different pH and temperature values.

3.2. SAXS data analysis

3.2.1. Theoretical SAXS curves obtained from Protein Data Bank (PDB) for HbLt

Theoretical SAXS curves were obtained from *L. terrestris* hemoglobin (HbLt) coordinate data deposited in the Protein Data Bank (PDB) under ID code 2GTL [7] by using Crysol software [18]. The architecture of the full particle of approximately 3.6 MDa is based on two hexagonal disks in which the most prominent substructure corresponds to one-twelfth of the whole particle (a protomer) which is composed of a dodecamer of globins, $(abcd)_3$, together with three non-globin chains called linkers, L_1, L_2, and L_3. Thus, assuming a high similarity of the three dimensional structure between HbGp and HbLt, we obtained the theoretical SAXS curves of the different subunits of the HbGp, based on the deposited coordinates for HbLt [7]. It is worthy of mention that a recent report [20] on the preliminary crystal structure of HbGp confirmed its close similarity to HbLt structure [7]. The theoretical scattering curves obtained from PDB structure, which were the most representative for analysis of our experimental SAXS scattering curves, will be discussed later into the text.

3.2.2. Independent-model data analysis

The scattering curves of HbGp at three different iron oxidation states, oxy-, met- and cyanomet-HbGp, were analyzed initially by Guinier law [15] and p(r) functions through GNOM program [17] to assess the corresponding values of the parameters R_g, D_{max} and I(0). The R_g values obtained from p(r) functions agree quite well with those obtained from Guinier plots.

3.2.3. Stability of HbGp oxidation forms in acidic medium

Fig. 2 shows a representative scattering curve for oxy-HbGp, 3.0 mg/ml, at pH 5.0, and 20 °C. HbGp SAXS curves are characterized by two well defined shoulders in the q region of 0.04 $Å^{-1}$ and 0.07 $Å^{-1}$ and a third one, not so pronounced, in the q region of 0.12 $Å^{-1}$. These shoulders are characteristic of extracellular giant hemoglobins as reported in previous work [1,9,22].

All three HbGp oxidation forms show very similar SAXS scattering curves in the acidic pH range, which are also similar to the native oligomeric protein at pH 7.0. It is worthy of notice that this native scattering curve is maintained in the whole studied temperature interval from 20 to 60 °C, suggesting a significant oligomeric stability of HbGp, at 3.0 mg/ml, in the acidic pH range. Another interesting observation is the protein precipitation at temperatures above 60 °C, precluding more detailed studies at higher temperatures. These results are quite consistent with previous DLS data [14]. In Fig. 2A the superposition of the experimental scattering curve with the theoretical curve obtained based on HbLt coordinates, as described above, is quite good. In Fig. 2B the pair distance distribution function, p(r), is shown, which is characteristic for the HbGp native state, with a D_{max} of 300 Å and a radius of gyration R_g of 107 Å [9]. Such a value of R_g is consistent with the hydrodynamic diameter of HbGp, obtained by DLS measurements, of 27(1) nm ($R_g = (\sqrt{3}/5) \times R$ for a sphere, [16]).

The parameters for all three forms of HbGp are reported in Tables 2–4. Inspection of the parameters for the acidic range is quite informative. For all different oxidation forms where dissociation is not observed, at 20 °C, the I(0) value is constant. This observation is consistent with data obtained from other experiments and suggests that the quaternary structure is similar regardless the protein oxidation form. For pH values of 5.0 and 6.0, at temperatures higher than 40–50 °C (see Tables 2–4), the I(0) values showed a slight decrease due to the initial protein precipitation. This result is in agreement with a recent paper [14] describing the isoelectric point determination of HbGp, which is around 5.5.

Besides, the *M* value obtained by SAXS MoW program was about 3.3 MDa for temperatures up to 40 °C, corresponding to the native whole oligomeric form of HbGp. Such a value is close to the

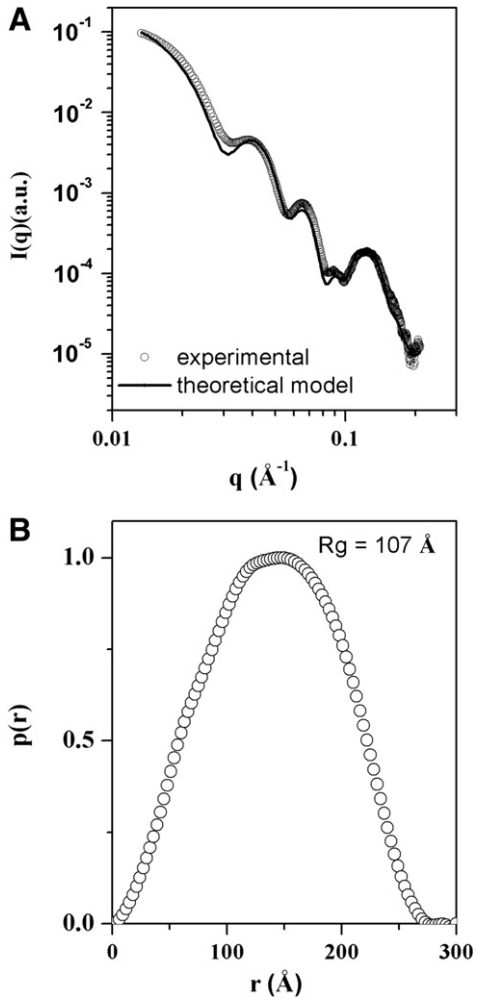

Fig. 2. Experimental small angle X-ray scattering curves of 3.0 mg/ml oxy-HbGp in 30 mM acetate–phosphate–borate buffer at pH 5.0, 20 °C and theoretical scattering curve obtained using the program CRYSOL [18] and based on the structure for HbLt deposited in the Protein Data Bank under ID code 2GLT [7] (A); normalized distance distribution function p(r) obtained from GNOM program.

Table 2
R_g, I(0) and D_{max} values obtained from GNOM software analysis for extracellular hemoglobin of *G. paulistus*, in the oxy-form, at indicated pH and temperature values.

T (°C)	Oxy-HbGp	pH 5.0	pH 6.0	pH 7.0	pH 8.0
20	R_g (Å)	107 ± 1	106 ± 1	108 ± 1	107 ± 1
	D_{max} (Å)	300	300	300	300
	I(0) (a.u.)	0.10 ± 0.01	0.10 ± 0.01	0.10 ± 0.01	0.10 ± 0.01
30	R_g (Å)	107 ± 1	107 ± 1	108. ± 1	106 ± 1
	D_{max} (Å)	300	300	300	300
	I(0) (a.u.)	0.10 ± 0.01	0.10 ± 0.01	0.10 ± 0.01	0.10 ± 0.01
40	R_g (Å)	106 ± 1	106 ± 1	108.6 ± 0.2	105 ± 1
	D_{max} (Å)	300	300	300	300
	I(0) (a.u.)	0.10 ± 0.01	0.10 ± 0.01	0.05 ± 0.01	0.07 ± 0.01
50	R_g (Å)	108 ± 1	106 ± 1	108 ± 1	104 ± 1
	D_{max} (Å)	300	300	300	280
	I(0) (a.u.)	0.10 ± 0.01	0.10 ± 0.01	0.03 ± 0.01	0.03 ± 0.01
55	R_g (Å)	107 ± 1	107 ± 1	137 ± 1	50 ± 1
	D_{max} (Å)	300	300	420	190
	I(0) (a.u.)	0.08 ± 0.01	0.09 ± 0.01	0.03 ± 0.01	0.003 ± 0.001
60	R_g (Å)	104 ± 1	105 ± 1	143 ± 1	50 ± 1
	D_{max} (Å)	300	300	450	190
	I(0) (a.u.)	0.08 ± 0.01	0.08 ± 0.01	0.012 ± 0.005	0.003 ± 0.001

Table 4
R_g, I(0) and D_{max} values obtained from GNOM software analysis for extracellular hemoglobin of *G. paulistus*, in the met-form, at indicated pH and temperature values.

T (°C)	Met-HbGp	pH 5.0	pH 6.0	pH 7.0	pH 8.0
20	R_g (Å)	107 ± 1	107 ± 1	107 ± 1	92 ± 1
	D_{max} (Å)	300	300	300	280
	I(0) (a.u.)	0.10 ± 0.01	0.10 ± 0.01	0.10 ± 0.01	0.010 ± 0.005
30	R_g (Å)	107 ± 1	107 ± 1	107 ± 1	90 ± 1
	D_{max} (Å)	300	300	300	295
	I(0) (a.u.)	0.10 ± 0.01	0.10 ± 0.01	0.10 ± 0.01	0.010 ± 0.005
40	R_g (Å)	106 ± 1	107 ± 1	107 ± 1	
	D_{max} (Å)	300	300	300	
	I(0) (a.u.)	0.10 ± 0.01	0.09 ± 0.01	0.09 ± 0.01	
50	R_g (Å)	107 ± 1	107 ± 1	105 ± 1	
	D_{max} (Å)	300	300	300	
	I(0) (a.u.)	0.09 ± 0.01	0.09 ± 0.01	0.07 ± 0.01	
60	R_g (Å)	106 ± 1	106 ± 1	122 ± 1	
	D_{max} (Å)	300	300	400	
	I(0) (a.u.)	0.09 ± 0.01	0.09 ± 0.01	0.04 ± 0.01	

experimental one obtained by analytical ultracentrifugation of 3.6 MDa [6]. As I(0) values suffer a slight decrease for higher temperatures, the resulting *M* values decrease from 3.3 MDa to 2.8 MDa, being certainly underestimated due to protein precipitation.

3.3. Stability of HbGp in neutral and alkaline media

3.3.1. Oxy-HbGp

Fig. 3A and B presents, respectively, the experimental scattering curves and distance distribution functions, p(r), as well as the corresponding scattering curves calculated by GNOM for oxy-HbGp, at pH 7.0 and pH 8.0. The R_g, D_{max} and I(0) values are included in Table 2. Similar to previous analysis, the HbGp keeps its native state up to 30 °C, with $M = 3.3$ MDa. However, at pH 7.0, I(0) decreases for temperatures above 40 and up to 50 °C, without changing in D_{max} and R_g values. Further temperature increase leads to an enlargement of the protein maximum dimension D_{max} that reaches 450 Å at 60 °C, pointing out the denaturation process followed by aggregation of the HbGp. The R_g value also increases to 143 Å, consistent with the shift of the maximum frequency in the distance distribution function p(r) (see dotted lines in Fig. 3A). Such apparent increase in scattering protein dimension due to HbGp aggregation precludes the real estimate of I(0) because the corresponding information is hidden in a q range not accessible by our experimental resolution. In this way, we cannot infer about the protein molecular weight at this experimental condition. Moreover, the reduction in I(0) could also be associated to the protein precipitation due to high protein aggregation, that is in agreement with our recently published paper [14], reporting significant precipitation at acidic pH, and moderate precipitation at pH 7.0.

At pH 8.0, a significant decrease of R_g and D_{max} to 50 Å and 190 Å, respectively, is observed starting at 55 °C, as oligomeric protein dissociation occurs, accompanied by a decrease in the forward scattering intensity I(0). This means that a decrease of approximately 5 times on I(0) is equivalent to the *M* value obtained. The protein molecular weight obtained by SAXS MoW software results to be 0.14 MDa. Thus, these results evidence the oligomeric dissociation of the oxy-HbGp at alkaline pH and high temperatures. As mentioned above, in the DLS data presentation, oligomeric dissociation of HbGp, at alkaline pH values, has been previously observed and well characterized. So, our present SAXS data for oxy-HbGp are consistent with previous DLS data [10,11].

3.3.2. Cyanomet-HbGp

At pH 7.0 (Fig. 4A), the protein is very stable, similar to the acidic pH range, maintaining the unchanged native scattering curve up to 60 °C, in good agreement with DLS data (see Table 1). For the cyanomet-HbGp form, the heme iron is oxidized being in the ferric state, and due to the coordination of the cyanide ion to the iron center, a significant oligomeric stability is achieved as a function of temperature. The values of D_{max} and R_g remain also constant in the whole temperature range, equal, respectively, to 300 and 108 Å (inset of Fig. 4A, Table 3). The values of *M* estimated by SAXS MoW remain constant and equal to 3.3 MDa.

However, at pH 8.0 (Fig. 4B), the protein is not as stable as at pH 7.0, practically loosing the characteristic shoulders at 60 °C and the

Table 3
R_g, I(0) and D_{max} values obtained from GNOM software analysis for extracellular hemoglobin of *G. paulistus*, in the cyanomet-form, at indicated pH and temperature values.

T (°C)	Cyanomet-HbGp	pH 5.0	pH 6.0	pH 7.0	pH 8.0	pH 9.0
20	R_g (Å)	107 ± 1	107 ± 1	107 ± 1	108 ± 1	107 ± 1
	D_{max} (Å)	300	300	300	300	300
	I(0) (a.u.)	0.10 ± 0.01	0.10 ± 0.01	0.10 ± 0.01	0.10 ± 0.01	0.07 ± 0.01
30	R_g (Å)	107 ± 1	107 ± 1	107 ± 1	108 ± 1	106 ± 1
	D_{max} (Å)	300	300	300	300	300
	I(0) (a.u.)	0.10 ± 0.01	0.10 ± 0.01	0.10 ± 0.01	0.10 ± 0.01	0.07 ± 0.01
40	R_g (Å)	107 ± 1	107 ± 1	108 ± 1	108 ± 1	106 ± 1
	D_{max} (Å)	300	300	300	300	300
	I(0) (a.u.)	0.09 ± 0.01	0.10 ± 0.01	0.09 ± 0.01	0.10 ± 0.01	0.06 ± 0.01
50	R_g (Å)	107 ± 1	107 ± 1	108 ± 1		75 ± 1
	D_{max} (Å)	300	300	300		245
	I(0) (a.u.)	0.09 ± 0.01	0.09 ± 0.01	0.09 ± 0.01		0.012 ± 0.001
60	R_g (Å)	107 ± 1	106 ± 1	108 ± 1	93 ± 1	
	D_{max} (Å)	300	300	300	250	
	I(0) (a.u.)	0.09 ± 0.01	0.09 ± 0.01	0.09 ± 0.01	0.02 ± 0.01	

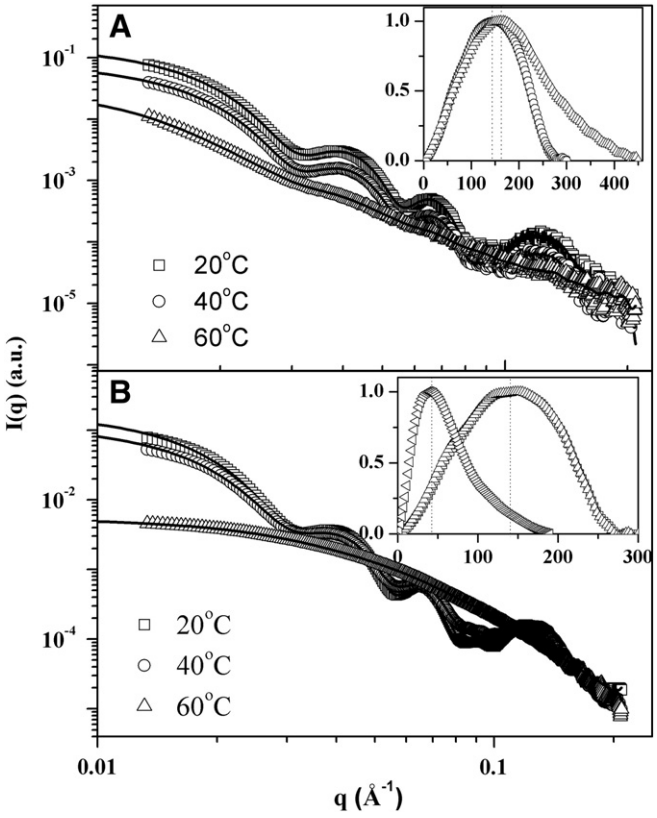

Fig. 3. Experimental small angle X-ray scattering curves of 3.0 mg/ml oxy-HbGp in 30 mM acetate–phosphate–borate buffer at pH 7.0 (A) and pH 8.0 (B) as a function of the temperature. The best normalized distance distribution functions p(r) obtained from GNOM program are included as insets on the figures and the corresponding scattering curves are represented as solid lines onto the experimental data.

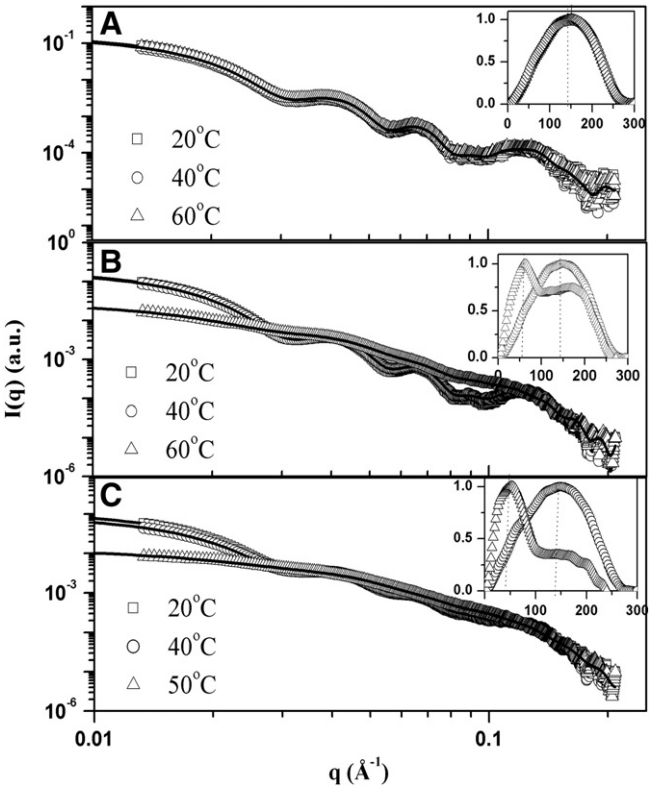

Fig. 4. Experimental small angle X-ray scattering curves of 3.0 mg/ml cyanomet-HbGp in 30 mM acetate–phosphate–borate buffer at pH 7.0 (A), pH 8.0 (B) and pH 9 (C) as a function of the temperature. The best normalized distance distribution functions p(r) obtained from GNOM program are included as insets on the figures and the corresponding scattering curves are represented as solid lines onto the experimental data.

corresponding values of D_{max} and R_g are reduced to, 250 and 93 Å, respectively (Table 3). The *M* value reduced from 3.3 MDa to 0.59 MDa due to the protein oligomeric dissociation. This dissociation of the whole oligomer into smaller subunits is also clearly seen in the inset of Fig. 4B showing a significant contribution of frequencies of smaller distances in the p(r) function corresponding to low molecular weight components (see dotted lines in the inset of Fig. 4B). Oligomeric dissociation for cyanomet-HbGp at pH 8.0 is also observed from our DLS data (Table 1).

At pH 9.0 (Fig. 4C), the SAXS curves show a clear further reduction of I(0) value already at 20 °C (see also Table 3). However, the three well defined shoulders in the q region of 0.04, 0.07 and 0.12 Å^{-1} are partially maintained up to 40 °C. At 50 °C the shoulders are practically absent, suggesting a reduction of thermostability of the cyanomet-HbGp form at this alkaline pH. D_{max} and R_g reduced, respectively, to 245 Å and 75 Å, at 50 °C (Table 3). Based on SAXS MoW analysis, at pH 9.0, the oligomeric dissociation is already observed at 20 °C since the *M* value reduces to 2 MDa. Increasing the temperature from 20 to 50 °C the *M* value reduces further to 0.27 MDa. Monitoring the changes in the p(r) function in going from pH 8.0 to pH 9.0 the reduction of the contribution at the higher pH of the higher molecular mass species and the simultaneous increase in the low molecular mass component contribution (see inserts of Fig. 4B and C, and dotted lines) are evident.

3.3.3. Met-HbGp

For the met-HbGp, at pH 7.0 (Fig. 5A), up to 40 °C the scattering curve with the characteristic shoulders is maintained and the initial scattering intensities decrease significantly above a temperature around 50 °C. I(0) reduces from 0.10 to 0.04 upon going from 20 °C to 60 °C (see Table 4). At 60 °C, a drastic change is observed (Fig. 5A), and the parameters D_{max} and R_g increased to 400 and 122 Å, respectively. The marked decrease in the initial scattering intensity is accompanied by the disappearance of the characteristic shoulders in the experimental scattering curve. For met-HbGp, at pH 7.0 above 40 °C, the *M* value was not determined due to protein precipitation. As mentioned above, at 20 °C the *M* value is equal to 3.3 MDa, the same as for native HbGp independent of oxidation form. The p(r) function at pH 7.0 (Fig. 5A) has a maximum of frequencies shifted toward r values smaller than those observed for oxy- and cyanomet-HbGp (Figs. 3A and 4A). It is possible that the met-form is more prone to undergo dissociation, prior to the aggregation, as compared to the other two forms. However, DLS data (Table 1) show that the denaturation temperature is lower as compared to the other forms, with no dissociation, and large aggregates are formed above this critical temperature. Therefore, such displacement of the distribution of frequencies in the p(r) function to smaller distances may be also correlated to some denaturation process followed by aggregation at T_{den} (Table 1).

The scattering curves for met-HbGp at pH 8.0 are shown in Fig. 5B. It is clearly observed that already at 20 °C the characteristic native structure with the shoulders is not observed, indicating extensive oligomeric dissociation. The values of D_{max}, R_g and I(0) are all consistent with this behavior: 280 Å, 92 Å and 0.01 a.u., respectively at 20 °C (Table 4). At pH 8.0, already at 20 °C, the value of *M* is reduced (0.27 MDa) as compared with the value at pH 7.0, indicating again the occurrence of the oligomeric dissociation process. In this way, our results point out that the oxidation state of the iron interferes significantly in the protein oligomeric dissociation: at the same pH the met-form of HbGp is more thermally unstable, as compared with the oxy- and cyanomet-forms.

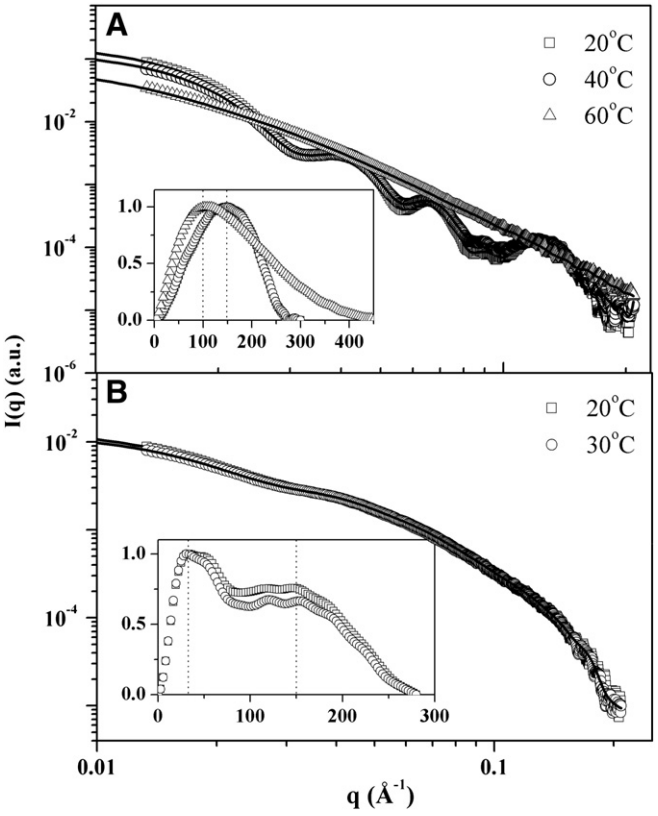

Fig. 5. Experimental small angle X-ray scattering curves of 3.0 mg/ml met-HbGp in 30 mM acetate–phosphate–borate buffer at pH 7.0 (A) and pH 8.0 (B) as a function of the temperature. The best normalized distance distribution functions p(r) obtained from GNOM program are included as insets on the figures and the corresponding scattering curves are represented as solid lines onto the experimental data.

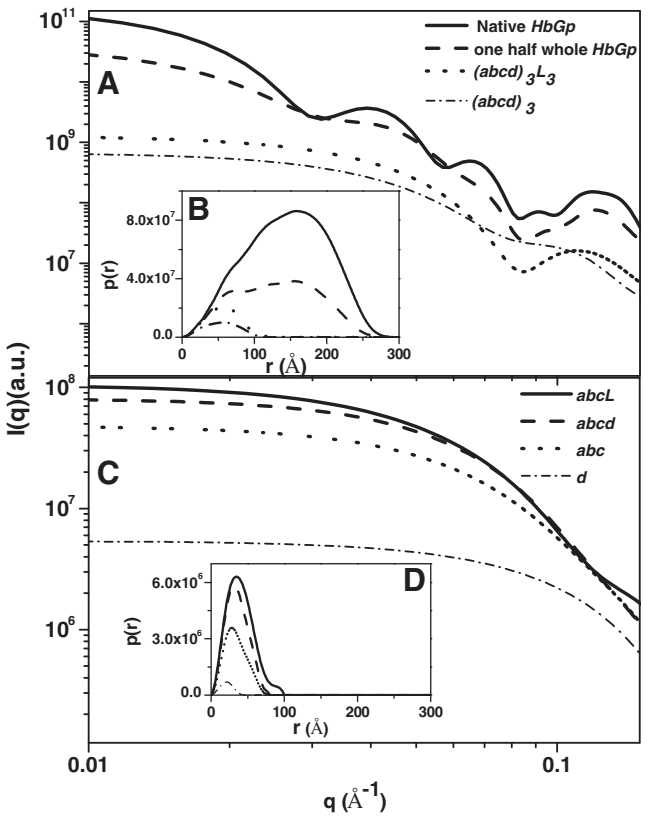

Fig. 6. Theoretical SAXS curves based on the structure for HbLt deposited in the Protein Data Bank under ID code 2GLT [7] obtained using the program CRYSOL [18]. Higher molecular mass fragments (A) and lower molecular mass fragments (C). Insets (B) and (D) correspond to the distance distribution function p(r) obtained from GNOM program.

3.4. Analysis of oligomeric dissociation of the HbGp

As described in the Materials and methods section, the program GNOM was used in the present study to obtain the distance distribution functions p(r) for each subunit based on the corresponding theoretical scattering curves for HbLt fragments. It should be stressed, however, that this is just a crude approximation since the HbLt theoretical scattering curves for the fragments are obtained as parts from the rigid body crystallographic structure that might not be exactly the same as the scattering for the corresponding fragments (subunits) in the aqueous solution, as is the case for the experimental curves. We also applied the OLIGOMER software to obtain fits for the experimental SAXS curves based on a linear combination of the theoretical scattering curves from HbLt fragments. In both fits, obtained either by p(r) from GNOM using *Origin* or directly from I(q) using OLIGOMER, the fragments corresponding to the lower molecular masses, associated to the globin trimers, monomers and some combinations including linkers (*abc*, *d*, *abc* + *L* and *abc* + *d*), were not considered, due to their very small scattering intensity contribution in respect to larger species. In fact, we tested initially the use of smaller fragments by using the OLIGOMER software, but their inclusion increased significantly the errors in the fragment contribution estimation without improving the quality of the fits. Moreover, the fits performed by using a linear combination of p(r) for the fragments, and based on the *Origin* software, were used as a starting point to have reasonable parameters as an initial guess for the fits by the OLIGOMER program.

In Fig. 6 the theoretical scattering curves for the HbLt fragments along with the corresponding p(r) functions (see insets) are shown. For clarity, the curves were split in two parts, emphasizing the greater (Fig. 6A) and the smaller (Fig. 6C) molecular mass subunits. The scattering intensities in Fig. 6A and C are not normalized and obey the corresponding mass relations. Moreover, the p(r) functions are normalized by the corresponding factor, assuming an HbGp stoichiometry of $12(abcd)_3L_3$ for the whole oligomer, aiming to facilitate the comparisons.

In order to better evaluate how the heat impacts on the dissociation process of different HbGp oxidation forms, the analysis through p(r) composition combined to OLIGOMER was performed for the proteins at different conditions of pH and temperature, as described below.

Fig. 7A shows the p(r) function obtained from the experimental scattering curve by GNOM, for oxy-HbGp, at pH 7.0 and 20 °C, and the corresponding fit (solid line) obtained by the linear combination of the HbLt fragments. The data were fitted, in this case, with 100% of the native whole protein. Inset in Fig. 7A shows the corresponding experimental scattering curve for oxy-HbGp in this condition and the fit by OLIGOMER software, which gives also 100% of the native form. In this way, for the native HbGp, which is a single species system, both the p(r) analysis and the OLIGOMER program present a reasonable description of the experimental data.

Fig. 7B shows the p(r) function obtained from GNOM, for oxy-HbGp, at pH 8.0 and 60 °C, and the corresponding fit obtained from the linear combination of the theoretical HbLt fragments (see Fig. 6), as described above. Using this procedure the following contributions are obtained: one half of the native whole protein, $6\times(abcd)_3L_3$ ($2\pm1\%$), dodecamer, $(abcd)_3$ ($48\pm13\%$), and tetramers, $(abcd)$ ($50\pm43\%$). This result is consistent with the fact that the experimental p(r) goes only up to 200 Å and the scattering curve lacks the oscillations characteristic of higher mass fragments. It is also clear that the p(r) for this condition presents a tail above 100 Å, corresponding, probably, to denatured protein. The fit shown in Fig. 7B was limited to 150 Å, since the extension of the distance range to

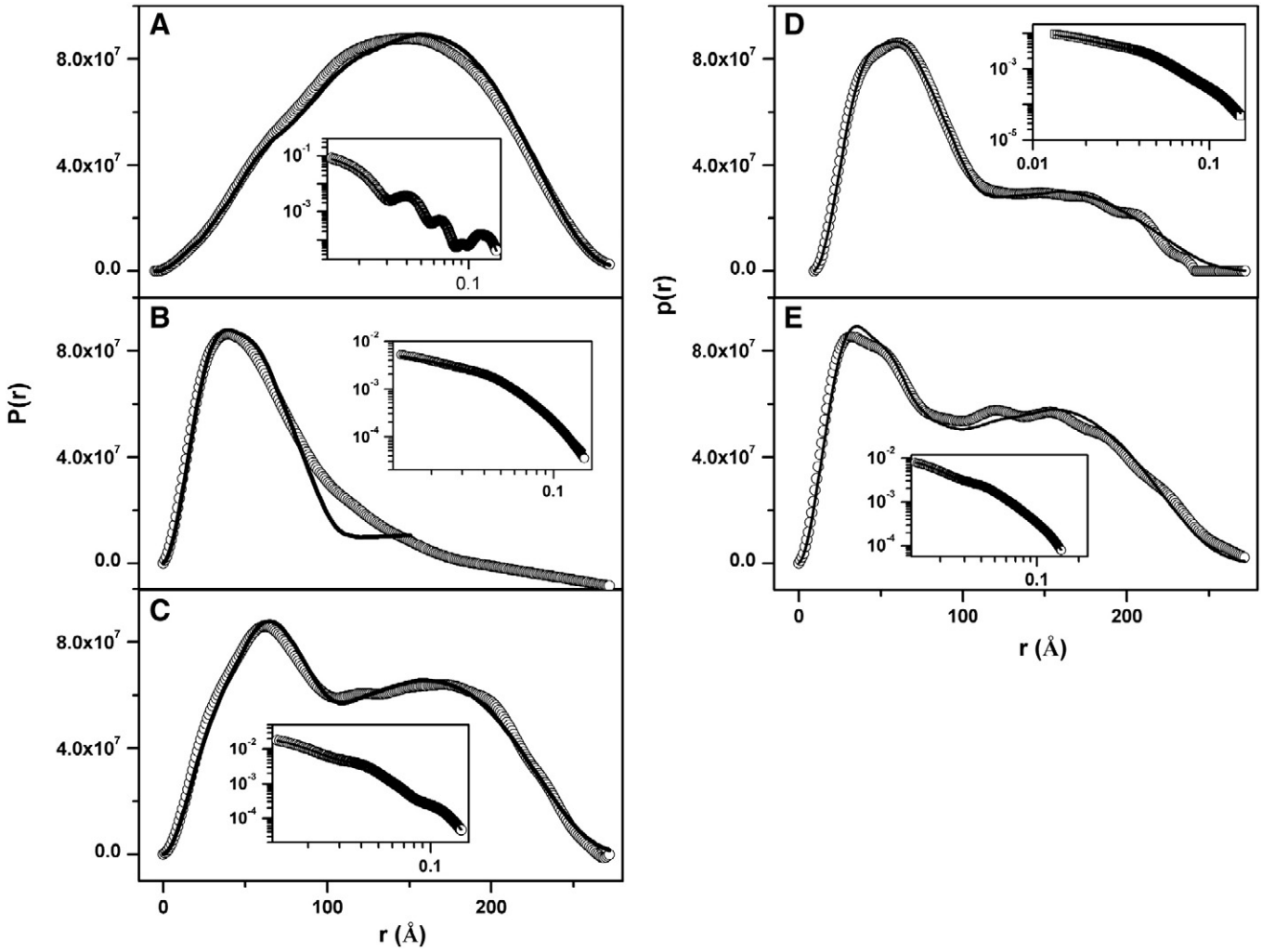

Fig. 7. Experimental SAXS curves and p(r) obtained for different HbGp oxidation forms. The electronic density distribution as function of distance p(r) obtained from GNON for experimental scattering curves and the better fit considering the p(r) of the theoretical scattering curves of the high resolution subunits from HbLt (*Lumbricus erythrocruorin*) deposited in the Protein Data Bank under ID code 2GTL [7]. (A) oxy-HbGp pH 7.0 and 20 °C (B) oxy-HbGp pH 8.0 and 60 °C, (C) cyanomet-HbGp, pH 8.0 and 60 °C, (D) cyanomet-HbGp, pH 9.0 and 50 °C, (E) met-HbGp, pH 8.0 and 30 °C. Insets present experimental SAXS I(q) (a.u.) vs q (Å) curves and fits from OLIGOMER [19]. The open circles correspond to the experimental points and the solid lines to the best fits.

190 Å would produce an averaging of the experimental curve in the higher r region, changing slightly the contributions, but maintaining these three species. The existence of this long distance tail precludes an improvement of the fit since the p(r) for denatured protein is unavailable. Thus, this result is only an approximation since the fit of the p(r) is not good enough at high values of r (Fig. 7B). Inset in Fig. 7B shows the same experimental scattering curve and the corresponding fit obtained by OLIGOMER. The best fit results in a combination of one half of the whole protein (5.3 ± 0.2%), the dodecamer $(abcd)_3$ (23 ± 1%), and the tetramer (*abcd*) (72 ± 1%). Both fits, obtained from the linear combination of the p(r) for the fragments, and by OLIGOMER, which uses in essence the same approach, show clearly a high contribution of dodecamer and tetramer, together with a few percent of half of the whole protein. All fitting results are collected together in Table 5.

Fig. 7C presents the analysis of scattering data for cyanomet-HbGp, at pH 8.0 and 60 °C. From the p(r) fitting, the following contributions are obtained: whole protein (11 ± 1%), 1/12 of the whole protein (6 ± 3%), dodecamer (61 ± 5%), and tetramer (22 ± 2%). This result is quite consistent with the inspection of both the scattering curve (inset of Fig. 7C) and p(r) function, where some oscillations and shoulder at high r values are, respectively, observed. It is also consistent with the fact that cyanomet-HbGp, at pH 8.0 and 60 °C, is more stable toward oligomeric dissociation as compared to oxy-HbGp (Fig. 7B). The fit obtained by OLIGOMER (inset of Fig. 7C) indicates that the experimental SAXS curve can be composed by native protein (13 ± 1%), 1/12 of the whole protein (12 ± 1%), the dodecamer (49 ± 1%), and the tetramer (26 ± 1%), showing that both fits are quite good giving consistent values for species contributions (see also Table 5).

Fig. 7D shows the p(r) obtained from GNOM for cyanomet-HbGp, at pH 9.0 and 50 °C, and the corresponding fit obtained by the linear combination of the theoretical curves for the HbLt fragments (Fig. 6). In this case the best fit shows contributions from one half of the whole protein (7 ± 1%), dodecamer (47 ± 4%), and tetramers (46 ± 1%). For cyanomet-HbGp, in going from pH 8.0 to pH 9.0, the contribution of higher mass species is reduced, and a significant increase in the amount of tetramers is observed (almost doubled). The fit obtained by OLIGOMER (inset of Fig. 7D) indicates the presence of the following subunits: one half of the whole protein (7.8 ± 0.2%), dodecamer (38 ± 1%), and tetramer (54 ± 1%). Again the contributions obtained from the two fits are quite consistent (Table 5).

Finally, for met-HbGp, at pH 8.0 and 30 °C (Fig. 7E and Table 5), analyses by p(r) indicated a contribution of native (2.0 ± 0.3%), one half of the whole protein (12 ± 1%), dodecamer (16 ± 8%), and the sum of trimers and monomers, *abc* + *d* (70 ± 26%). The results based

Table 5
Percentages contributions of fragments of the whole protein, obtained from linear combination of corresponding theoretical p(r) curves, and from OLIGOMER analysis, for the oxy-, cyanomet- and met-HbGp forms, at pH 7.0, 8.0 and 9.0, at indicated temperatures.

	Oxy-HbGp				Cyanomet-HbGp				Met-HbGp	
	pH 7.0		pH 8.0		pH 8.0		pH 9.0		pH 8.0	
	20 °C		60 °C		m		50 °C		30 °C	
Fragments	%p(r)	%OLIG.	%p(r)	%OLIG.	%p(r)	%OLIG.	%p(r)	%OLIG.	%p(r)	%OLIG.
Native	100%	100%	–	–	11 ± 1	13 ± 1	–	–	2.0 ± 0.3	1 ± 1
$6\times(abcd)_3L_3$	–	–	2 ± 1	5.3 ± 0.2	–	–	7 ± 1	7.8 ± 0.2	12 ± 1	11 ± 1
$1/12(abcd)_3L_3$	–	–	–	–	6 ± 3	12 ± 1	–	–	–	–
$(abcd)_3$	–	–	48 ± 13	23 ± 1	61 ± 5	49 ± 1	47 ± 4	38 ± 1	16 ± 8	16 ± 1
$(abcd)$	–	–	50 ± 43	72 ± 1	22 ± 2	26 ± 1	46 ± 1	54 ± 1	–	–
$abc+d$	–	–	–	–	–	–	–	–	70 ± 26	72 ± 1

%p(r) — percentages obtained by linear combination using p(r) fragments of the HbLt shown in Fig. 6.
%OLIG. — percentages obtained by OLIGOMER program.
Native protein corresponds to 12 protomers $(abcd)_3L_3$, one half of the native protein corresponds to 6 protomers $(abcd)_3L_3$, dodecamer $(abcd)_3$, tetramers *abcd*, sum of trimer and monomer $(abc+d)$ fragments.

on p(r) analysis are again quite consistent with the fact that met-HbGp, at pH 8.0, is quite unstable already at 20 °C, where a significant amount of lower mass components is observed, leaving only 30% of higher mass components. As mentioned above, this is just an approximation for the estimates of species contributions. We believe that despite the limitations of this analysis, for comparative purposes regarding the pH and temperature effects, it can be useful. OLIGOMER fit indicated the contribution of the whole protein (1 ± 1%), one half of the whole protein (11 ± 1%), dodecamer (16 ± 1%), and the sum of trimer and monomer, $abc+d$ (72 ± 1%). In this case the quality of the fit has been quite improved upon the choice of the scattering curve resulting from the sum of trimer and monomer instead of using the tetramer. It is possible that this is associated also to the higher tendency of met-HbGp to completely dissociate at pH 8.0.

4. General discussion

In the last 10 years the number of studies aiming to obtain structural information for different proteins based on the SAXS technique has increased [23–29]. This technique allows following changes on the tridimensional protein structure, monitoring the solution under controlled conditions of salts, substrates, co-factors, etc., which mimics closely the biological environment involved with the protein function. In a favorable situation, it is possible to study the equilibrium among different species in solution based on their molecular mass. Most of these studies in the literature reports protein denaturation induced by high concentrations of denaturing agents [30], by rising the temperature [26], changing the pH [25], or even the ionic strength [28], as well as, describes the process of oligomeric dissociation and aggregation [24].

Interestingly, Spinozzi et al. [28] studied the effects of GuHCl and NaCl on the structural properties of the hemocyanin (Hc) from *Carcinus aestuarii*, at different conformational states: hexameric holo- and apo-Hc forms, as well as the holo- and apo-forms of the monomeric subunit *Cae*SS2, by means of small angle X-ray scattering (SAXS). By analyzing the data, assuming equilibrium of different species in solution (GENFIT software), the authors evidenced that the presence of small amounts of GuHCl (up to 1.25 M) was not able to disrupt the hexameric holo-Hc form, which is ~92% of total Hc in solution. Increasing GuHCl concentration, however, in the range of 1.25–2.50 M, higher aggregated forms, like dodecamers and icosatetramers, were observed. At concentrations higher than 2.5 M GuHCl, the authors evidenced a complete dissociation of the protein, followed by an unfolding process. A different effect was observed in the presence of NaCl, were no dissociation or aggregation processes were observed up to 3 M NaCl. Therefore, SAXS is a suitable technique to study protein–protein dissociation and/or aggregation, as well as folding/unfolding processes.

However, many of the studies found in the literature are performed with monomeric and homo-dimeric proteins that are very simple systems, where the determination of the species in solution can be performed with the use of softwares, such as, OLIGOMER, SAXS MoW and GNOM [17–19]. Besides, using other programs such as CRYSOL [18], it is possible to generate theoretical SAXS curves corresponding to either a fragment or to the whole crystallographic structure of a protein.

In a recent paper, Shang et al. [23] described the dimerization process and the structural flexibility of mammalian lipoxygenases. This enzyme is characterized by a dimer, consisting of two structurally different monomeric conformers A and B. Guinier plot analysis yields a radius of gyration R_g of 49 Å, and a particle volume of 300×10^3 Å^3, corresponding to a molecular mass of 150 kDa. This mass corresponds to a dimer, which in the crystal structure presents smaller R_g (41 Å) and D_{max} (145 Å) values, explained by the authors as due to a different degree of motional flexibility in the crystal as compared to the solution. A monomer–dimer equilibrium was suggested, with a shift toward dimer formation at higher protein concentrations.

The protein aggregation state can be followed through the analysis of the changes of the forward scattering intensity I(0), as a function of external parameters, such as the temperature or addition of denaturants. For an ensemble of monomeric proteins of number density *n* and known electron density contrast Δρ, I(0) is directly proportional to the square of the protein volume V_P. In the case of monomeric self-aggregation giving N monomers in the aggregate, the scattering protein number density decreases by a factor of N, while the resulting scattering protein volume increases to $(NV_P)^2$. In this way I(0) increases by a factor of N and carries the information regarding the multimeric state of the protein in solution, such that $I(0)=N(\Delta\rho)^2nV_P^2$. This means that the I(0) for a homo-dimer and homo-tetramer is expected to increase by a factor of 2 and 4, respectively, as compared to the monomer [29]. An interesting system behaving in this way is the lectin peanut agglutinin (PNA) [27]. The theoretical SAXS scattering curves, based on the crystallographic structure obtained for the homo-tetrameric native protein, as well as for the monomer and homo-dimer subunits, were in very good agreement with the corresponding experimental curves and expected I(0) relations.

Certainly, for more complex protein oligomeric structures, such as, for example, a hetero-trimer and/or a hetero-hexamer, the characterization of the solution species in equilibrium has proven to be significantly more difficult, as compared to the previous simple monomer, homo-dimer and homo-tetramer situation. De Marco et al. [28] in a study of human Cdt1-germin and its mutant forms, have shown the existence of hetero-trimer (44 kDa) and hetero-hexamer (88 kDa) structures. However, in this case, the theoretical scattering curve is significantly different as compared to the experimental one. In this way, for complex structures, the analysis of SAXS data based on the crystal structures is not always completely successful.

The description made above does not work with HbGp since the aggregates and oligomeric fragments do not correspond to simple monomers, dimers or tetramers of these monomers. The HbGp system is quite complex. In this context, another recent investigation shows that the complexity of the HbGp oligomeric dissociation process is, at least partially, related to the difficulties in the characterization of its isolated subunits, through size exclusion chromatography (SEC), electrophoresis and MALDI-TOF-MS studies [31]. SEC studies, at pH 9.6, show that oxy-HbGp undergoes oligomeric dissociation, producing smaller subunits/fragments, such as, the dodecamer, the trimer, the linkers and the monomer. Moreover, electrophoresis experiments show that the linker subunits contaminate the trimer fraction, implying a high affinity of the linkers to the trimer, preventing the complete separation of these subunits. As mentioned above in the Introduction, at pH 10.0, ultracentrifugation studies presented a complex equilibrium of small molecular weight species without the clear presence of the linkers [8]. Hydrodynamic properties of HbLt fragments, obtained from the crystal structure, were also simulated in this work, giving interesting results: the properties of the isolated linker chains in different aggregation states (monomers, dimers and trimers) are quite similar to HbGp globin monomers and dimers of monomers, making their separation into pure form difficult [8].

Regarding the analysis of the SAXS data obtained in the present work for HbGp, at different pH values, some care is necessary since the behavior of the protein in acidic pH range, at pH 7.0 and in alkaline medium is rather different. For instance, in acidic pH, the denaturation temperature is known to be higher as compared to pH 7.0 [11,14] and the aggregation phenomenon that occurs after denaturation is more intense, probably, due to the proximity of the protein isoelectric point, which is around 5.5 [14]. At pH 7.0, the protein undergoes denaturation forming somewhat smaller aggregates than in the acidic medium, as mentioned above. The physical visible precipitation is also not so strong, at pH 7.0, as compared to the acidic pH range. Furthermore, in alkaline solution the oligomeric dissociation takes place with increase of temperature, producing some mixtures of fragments of the whole protein (subunits) with different volumes and molecular masses. All these phenomena contribute to make it more difficult the analysis of the HbGp denaturation process by SAXS.

Despite all the difficulties, mentioned above, to find an adequate model that describes HbGp temperature-induced dissociation/denaturation, we believe that our present studies are an important advance on the analysis and on the understanding of the protein denaturation. Moreover, in this work, estimates of the percentage contribution to the experimental scattering curves of some fragments of the whole protein were obtained, for several characteristic fragments such as, for example, half of the protein corresponding to a single hexagonal layer, the one-twelfth of the whole protein ($(abcd)_3L_3$), corresponding to one of the twelve protomers composing the hexagonal bilayer, the dodecamer ($abcd)_3$, and either the tetramer ($abcd$) or a combination of the trimer (abc) and the monomer (d), as discussed above (see Table 5).

Further work is still needed to establish a reliable model for oligomeric dissociation of HbGp under different conditions of pH, protein concentration and temperature that would explain the extensive spectroscopic and structural data accumulated until now. Work is presently under way in our laboratory to characterize the different aggregate species, obtained in the presence of the denaturant urea, in different concentrations based in ultracentrifugation studies. However, we believe that our present SAXS data, despite the limitations of the technique that is not able to separate isolated contributions, being very sensitive to very small amounts of larger particles, is a nice contribution, highlighting that even at high temperatures a fraction of half of the whole molecule, as well as of the protomer (1/12 of the whole oligomer), the dodecamer and the tetramer remains in solution contributing to the total scattering.

5. Conclusions

In this work, the stability of the HbGp in different oxidation forms was studied in terms of different pH values and temperatures. DLS results show that the protein oligomeric dissociation and denaturation/aggregation are dependent on the protein concentration. Cyanomet-HbGp shows higher critical denaturation and dissociation temperatures, as observed from the melting curves, consistent with its higher stability as compared to oxy- and met-HbGp.

SAXS studies of cyanomet-HbGp, at pH 7.0, as a function of temperature, in the range 20–60 °C, show great protein stability. Our results suggest that cyanomet-form is more stable and resistant regarding oligomeric dissociation than met- and oxy-HbGp. Different analyses were performed in this work aiming to better characterize the process of HbGp dissociation. The oligomeric dissociation induced by temperature and alkaline pH for cyanomet-HbGp is not complete, which is in agreement with the results obtained by the other techniques. Besides that, our study evidences the high complexity of this oligomeric system due, probably, to the existence of different combinations involving both globin chains, as well as, linker chains that can interact as the oligomer is dissociated. Consequently, this implies that simple stoichiometric models are not enough to describe the species in equilibrium in solution upon dissociation. In critical conditions, at alkaline pH and higher temperature values our results indicated that, independent of the iron oxidation form, the species present in the equilibrium upon oligomeric dissociation are similar. The analysis by linear combination from p(r) and OLIGOMER program shows that, upon oligomeric dissociation, the percentage contributions of the subunits, such as, the dodecamer $(abcd)_3L_3$ and the tetramer ($abcd$), increase with temperature. On the other hand, the percentage of the heavier species, un-dissociated protein, one half of whole protein and one-twelfth of whole protein, present a significant decrease, with increasing of temperature and pH. The data are in agreement with recent results obtained by analytical ultracentrifugation, at alkaline pH.

Acknowledgments

The authors are indebted to the Brazilian agencies FAPESP, CNPq and CAPES for partial financial support. P. S. Santiago is grateful to CNPq and FAPESP for financial support. M. Tabak and R. Itri are recipients of research fellowships from CNPq. J.W.P. Carvalho is a recipient of a PhD. grant from FAPESP (2010/09719-0). The authors are also indebted to the staff of the SAXS beamline at LNLS, Campinas, Brazil for help with the SAXS experiments. Thanks are due to Mr. Ézer Biazin for excellent help with HbGp sample preparations.

Appendix A. Supplementary data

Supplementary data to this article can be found online at doi:10.1016/j.bpc.2012.02.004.

References

[1] A. Krebs, J. Lamy, S.N. Vinogradov, P. Zipper, *Lumbricus terrestris* hemoglobin: a comparison of small angle X-ray scattering and cryoelectron microscopy data, Biopolymers 45 (1998) 289–298.
[2] S.N. Vinogradov, The stoichiometry of the four linker subunits of *Lumbricus terrestris* hemoglobin suggests an asymmetric distribution, Micron 35 (2004) 127–129.
[3] J.N. Lamy, B.N. Green, A. Toulmond, J.S. Wall, R.E. Weber, S.N. Vinogradov, Giant hexagonal bilayer hemoglobins, Chemical Reviews 96 (1996) 3113–3124.
[4] R.E. Weber, S.N. Vinogradov, Nonvertebrate hemoglobins: functions and molecular adaptations, Physiological Reviews 81 (2001) 570–611.
[5] M. Rousselot, D. Le Guen, C. Chabasse, F. Zal, Novel dissociation mechanism of a polychaetous annelid extracellular haemoglobin, FEBS Journal 273 (2006) 1582–1596.
[6] F.A.O. Carvalho, P.S. Santiago, J.C. Borges, M. Tabak, On the molecular mass of extracellular hemoglobin of *Glossoscolex paulistus*: analytical ultracentrifugation reexamination, Analytical Biochemistry 385 (2009) 257–263.

[7] W.E. Royer, H. Sharma, K. Strand, J.E. Knapp, B. Bhyravbhatla, *Lumbricus erythrocruorin* at 3.5 Angstrom resolution: architecture of a megadalton respiratory complex, Structure 14 (2006) 1167–1177.
[8] F.A.O. Carvalho, P.S. Santiago, J.C. Borges, M. Tabak, Molecular masses and sedimentation coefficients of extracellular hemoglobin of *Glossoscolex paulistus*: alkaline oligomeric dissociation, International Journal of Biological Macromolecules 48 (2011) 183–193.
[9] E.L. Gelamo, R. Itri, M. Tabak, Small angle X-ray scattering (SAXS) study of the extracellular hemoglobin of *Glossoscolex paulistus*. Effect of pH, iron oxidation state, and interaction with anionic SDS surfactant, Journal of Biological Chemistry 279 (2004) 33298–33305.
[10] P.S. Santiago, J.W.P. Carvalho, M.M. Domingues, N.C. Santos, M. Tabak, Thermal stability of extracellular hemoglobin of *Glossoscolex paulistus*: determination of activation parameters by optical spectroscopic and differential scanning calorimetric studies, Biophysical Chemistry 152 (2010) 128–138.
[11] P.S. Santiago, F. Moura, L.M. Moreira, M.M. Domingues, N.C. Santos, M. Tabak, Dynamic light scattering and optical absorption spectroscopy study of pH and temperature stabilities of the extracellular hemoglobin of *Glossoscolex paulistus*, Biophysical Journal 94 (2008) 2228–2240.
[12] S.C.M. Agustinho, M.H. Tinto, J.R. Perussi, M. Tabak, H. Imasato, Fluorescence studies of extracellular hemoglobin of *Glossoscolex paulistus* in met form obtained from sephadex gel filtration, Comparative Biochemistry and Physiology 118A (1998) 171–181.
[13] S.C.M. Agustinho, M.H. Tinto, H. Imasato, T.T. Tominaga, J.R. Perussi, M. Tabak, Spectroscopic studies of the met form of the extracellular hemoglobin from *Glossoscolex paulistus*, Biochimica et Biophysica Acta 1298 (1996) 148–158.
[14] P.S. Santiago, F.A.O. Carvalho, M.M. Domingues, N.C. Santos, M. Tabak, Isoelectric point determination for *Glossoscolex paulistus* extracellular hemoglobin: oligomeric stability in acidic pH and relevance to protein–surfactant interactions, Langmuir 26 (2010) 9794–9801.
[15] A. Guinier, G. Fournet, Small Angle Scattering of X-rays, Wiley, New York, 1955.
[16] O. Glatter, O. Kratky, Small Angle X-ray Scattering, Academic Press, London, 1982.
[17] D.I. Svergun, Mathematical-methods in small-angle scattering data-analysis, Journal of Applied Crystallography 24 (1991) 485–492.
[18] P.V. Konarev, M.V. Petoukhov, V.V. Volko, D.I. Svergun, ATSAS 2.1, a program package for small-angle scattering data analysis, Journal of Applied Crystallography 39 (2006) 277–286.
[19] H. Fisher, M. De Oliveira Neto, H.B. Napolitano, I. Polikarpov, A.F. Craievich, The molecular weight of proteins in solution can be determined from a single SAXS measurement on a relative scale, Journal of Applied Crystallography 43 (2010) 101–109.
[20] J.F.R. Bachega, L. Bleicher, E.R. Horjales, P.S. Santiago, R.C. Garratt, M. Tabak, Crystallization and preliminary structural analysis of the giant haemoglobin from *Glossoscolex paulistus* at 3.2, Journal of Synchrotron Radiation 18 (2011) 24–28.
[21] C.B. Cabral, H. Imasato, J.C. Rosa, H.J. Laure, C.H.T.P. Silva, M. Tabak, R.C. Garratt, L.J. Greene, Fluorescence properties of tryptophan residues in the monomeric d-chain of *Glossoscolex paulistus* hemoglobin: an interpretation based on a comparative molecular model, Biophysical Chemistry 97 (2002) 139–157.
[22] A. Krebs, P. Zipper, S.N. Vinogradov, Lack of size and shape alteration of oxygenated and deoxygenated *Lumbricus terrestris* hemoglobin? Biochimica et Biophysica Acta 1297 (1996) 115–118.
[23] W. Shang, I. Ivanov, D.I. Svergun, O.Y. Borbulevych, A.M. Aleem, S. Stehling, J. Jankun, H. Kühn, E. Skrzypczak-Jankun, Probing dimerization and structural flexibility of mammalian lipoxygenases by small-angle X-ray scattering, Journal of Molecular Biology 409 (2011) 654–668.
[24] L. Giehn, D.I. Svergun, D.E. Otzen, B. Vestergaard, Low-resolution structure of a vesicle disrupting α-synuclein that accumulates during fibrillation, Proceedings of the National Academy of Sciences of the United States of America 108 (2011) 3246–3251.
[25] J. Pérez, P. Vachette, D. Russo, M. Desmadril, D. Durand, Heat-induced unfolding of neocarzinostatin, a small all-β protein investigated by small-angle X-ray scattering, Journal of Molecular Biology 308 (2001) 721–743.
[26] S. Ayuso-Tejedor, R. García-Fandiño, M. Orozco, J. Sancho, P. Bernado, Structural analysis of an equilibrium folding intermediate in the apoflavodoxin native ensemble by small-angle scattering, Journal of Molecular Biology 406 (2011) 604–619.
[27] P.T. Campana, L.R.S. Barbosa, R. Itri, Conformational stability of peanut agglutinin using small angle X-ray scattering, International Journal of Biological Macromolecules 48 (2011) 398–402.
[28] V. De Marco, P.J. Gillespie, A. Li, N. Karantzelis, E. Christodoulou, R. Klompmaker, S. van Gerwen, A. Fish, M.V. Petoukhov, M.S. Iliou, Z. Lygerou, R.H. Medema, J.J. Blow, D.I. Svergun, S. Taraviras, A. Perrakis, Quaternary structure of the human Cdt1-Geminin complex regulates DNA replication licensing, Proceedings of the National Academy of Sciences of the United States of America 106 (2009) 19807–19811.
[29] L.R.S. Barbosa, F. Spinozzi, P. Mariani, R. Itri, (in press).Small angle X-ray scattering applied to proteins in solution, Chapter in the book Proteins in solution and at interfaces: Methods and Applications in Biotechnology and Materials Science, Wiley Series, editors: Juan Ruso & Ángel Piñeiro.
[30] F. Spinozzi, E. Maccioni, C.V. Teixeira, H. Amenitsch, R. Favilla, M. Goldoni, P. Di Muro, B. Salvato, P. Mariani, M. Beltramini, Synchrotron SAXS studies on the structural stability of *Carcinus aestuarii* hemocyanin in solution, Biophysical Journal 85 (2003) 2661–2672.
[31] F.A.O. Carvalho, J.W.P. Carvalho, P.S. Santiago, M. Tabak, Further characterization of the subunits of the giant extracellular hemoglobin of *Glossoscolex paulistus* (HbGp) by SDS-PAGE electrophoresis and MALDI-TOF-MS, Process Biochemistry 46 (2011) 2144–2151.